DOI: 10.53660/CLM-2089-23P37

Production of materials $LaMO_3$ (M= Mn, Fe, Co or Ni) and application as adsorbent for the removal of the turquoise blue dye

Produção de materiais $LaMO_3$ (M= Mn, Fe, Co ou Ni) e aplicação como adsorvente para remoção do corante azul turquesa

Received: 2023-09-10 | Accepted: 2023-10-15 | Published: 2023-10-20

Jéssica Aline Santos Lemos
ORCID: https://orcid.org/0000-0003-2098-6084
Programa de Pós-graduação em Química, Universidade Federal de Sergipe. Brasil
E-mail: jessicaalinesantoslemos@gmail.com
Júlia Botti Ridrigues Fernandes
ORCID: https://orcid.org/0009-0005-8707-8162
Programa de Pós-graduação em Química, Universidade Federal de Sergipe. Brasil
E-mail: juliaspn2@gmail.com
Ana Carla Batista de Jesus
ORCID: https://orcid.org/0000-0002-2619-2587
Programa de Pós-graduação em Física, Universidade Federal de Sergipe. Brasil
E-mail: carlabatista.ita@gmail.com
Marcelo José Barros de Souza
ORCID: https://orcid.org/0000-0001-6703-1547
Departamento de Engenharia Química, Universidade Federal de Sergipe. Brasil
E-mail: mjbsufs@gmail.com
Anne Michelle Garrido Pedrosa
ORCID: https://orcid.org/0000-0002-2991-8064
Programa de Pós-graduação em Química, Universidade Federal de Sergipe. Brasil
E-mail: annemgp@gmail.com

ABSTRACT

In this work, the effect of the type of metal in $LaMO_3$-type materials (M = Mn, Fe, Co or Ni) prepared by the milling method was studied, in the phase formation and the use as an adsorbent for removal of turquoise blue dye. The results indicated that all materials obtained contain $LaMO_3$ phase with perovskite structure as the main phase, presenting high thermal stability, besides pores and particles of different sizes and models. The pH of the zero load point values is close to 7.0, except for the material $LaFeO_3$. The materials were applied as adsorbents in the removal of the turquoise blue dye in an aqueous solution, showing removal efficiency in the range of 51 to 97%, with a time of about 30 minutes to reach adsorption equilibrium. Kinetic studies showed that the experimental data fit better to the variable constants model.

Keywords: Perovskite; Milling method; Adsorption; Turquoise blue.

RESUMO

Neste trabalho foi estudado o efeito do tipo de metal em materiais do tipo $LaMO_3$ (M = Mn, Fe, Co ou Ni) preparados pelo método de moagem, na formação de fases e na utilização como adsorvente para remoção do corante azul turquesa. Os resultados indicaram que todos os materiais obtidos contêm a fase $LaMO_3$ com estrutura perovskita como fase principal, apresentando alta estabilidade térmica, além de poros e partículas de diferentes tamanhos e modelos. O pH dos valores do ponto de carga zero é próximo de 7,0, exceto para o material $LaFeO_3$. Os materiais foram aplicados como adsorventes na remoção do corante azul turquesa em solução aquosa, apresentando eficiência de remoção na faixa de 51 a 97%, com tempo de cerca de 30 minutos para atingir o equilíbrio de adsorção. Estudos cinéticos mostraram que os dados experimentais se ajustam melhor ao modelo de constantes variáveis.

Palavras-chave: Perovskita; Método da moagem; Adsorção; Azul turquesa.

INTRODUCTION

The progressive population increase has exposed the environment to different forms of contamination. Among them, the most worrying concerns water bodies, which have been affected by different agents harmful to the environment and human health. Among the main pollutants are dyes, herbicides and pharmacological compounds (MANJUNATHAA et al., 2019; MAHMOODI et al., 2007).

The growing industrial activity requires the advancement of new techniques that seek low costs and efficiency in the manufacture of new materials developed, as well as decreasing environmental impacts, since the population is gradually more rigorous and concerned with the processes used in the production of products that end up harming nature. At this juncture, interests encompass the search for new paths for materials for industrial applications, such as adsorbents and catalysts (GARBA et al., 2020; JUNIOR et al., 2018; GRABOWSKA, 2016; MOURE; PEÑA, 2015; NASCIMENTO et al., 2021; LEMOS et al., 2023).

Currently, there is a range of natural or synthetic materials being used as adsorbents, from the most common ones such as silica gel, activated carbon and chitosan, to the most modern ones such as carbon nanotubes, titania nanoparticles, immobilized enzymes and quaternary ammonium salt (MAHMOODI et al., 2011; NGAH et al., 2011;OVEISI et al., 2019; MOHAJERSHOJAEI et al., 2015).

Materials with a perovskite structure are crystalline materials that can be classified as mixed oxides with the general formula ABO_3. In this structure, the A position is occupied by metal ions with large atomic radii such as those of block 1, block 2 and rare pile of earths, the B position generally comprises cations with smaller atomic radii, such as the d transition metals. In general, the metal that occupies position A promotes mechanical resistance to perovskites, while the metal that occupies position B provides ease of interaction in redox reactions (GARBA et al., 2020; JUNIOR et al., 2018; GRABOWSKA, 2016; MOURE; PEÑA, 2015).

Some relevant research has described the preparation of materials with perovskite structure, since they are multifunctional materials exhibiting magnetic, electrical, optical, thermal, catalytic, and adsorptive properties, among others, being also easy to obtain. The efficiency of this type of mixed oxide in specific applications may be related to several factors, among them the method of synthesis and the type of metal used in the B site. Studies focusing on synthesis, characterization, and application showed good results using perovskites containing Mn, Fe, Co and, Ni at site B. The results indicate that the activities of these materials will depend on the peculiarities of the application, composition, and synthesis method (GARBA et al., 2020; JUNIOR et al., 2018; GRABOWSKA, 2016; MOURE; PEÑA, 2015; NASCIMENTO et al., 2021; LEMOS et al., 2023; SOUZA et al., 2021; WANG et al., 2016; GALLEGO et al., 2013). Applications on the removal of dyes have also focused on the use of materials with perovskite structure with adsorbent properties, where good results were found using $LaMnO_3$, $LaFeO_3$, $LaCoO_3$ and, $LaNiO_3$ in the removal of dyes such as methylene blue, Congo red, rhodamine B and reactive black 5 (NASCIMENTO et al., 2021; LEMOS et al., 2023; LEMOS, 2022;SOUZA et al., 2021; PANAHI et al., 2017; MAHMOUDI et al., 2019; DENGA et al., 2019; PALAS et al., 2018). For some of the works, the $LaNiO_3$ material showed higher removal efficiency (LEMOS et al., 2023; SOUZA et al., 2021; GARBA et al., 2020).

Different synthesis routes have been developed in recent years in order to produce materials with perovskite structure and with the best characteristics such as: larger surface areas, higher crystallinity, smaller crystallites, etc. All these proposed routes are intended to produce structures that contribute to the development of perovskites with the best characteristics in order to be used in specific aplications. It is worth noting that each method has its particularity, in which it has different advantages and disadvantages, and it is up to the researcher to adopt the one that is most advantageous for its structure and application (BOLARÍN et al., 2007; CRISTÓBAL et al., 2009).

The milling method has been applied in the production of materials with perovskite structure and also in obtaining other materials such as biochar, polymer composite and metal hydride. This synthesis mechanism presents some advantages concerning the more commonly used solutions-based processes, such as lower toxicity, avoiding organic solvents, which may result in an adequate level of control over the stoichiometry of the final products, the ease of implementation that allows better mixing of reagents and can be leading to the formation of finer particles with a large surface area and a low amount of by-products. All these benefits have made the method widely studied for the synthesis of new materials (ZHANG; LV, 2020; PALAZON et al., 2020; LYU et al., 2018; CRISTÓBAL et al., 2009).

Chemical pollutants from domestic and industrial disposal have become a major concern in recent years. Certain industrial segments, such as textiles and foodstuffs, have a high drawback in their production methods: the presence of dyes in their wastewater (HOLKAR et al., 2016).

The volume of this type of tailings has grown proportionally nowadays due to population growth and the development of society. Associated with this is also the treatment type of this type of effluent, which ends up compromising the environment in the vicinity of these industries (HOLKAR et al., 2016).

Textile dyes are organic compounds that have complex aromatic structures, generally consisting of a chromophore group, responsible for the color, and auxiliary groups, responsible for fixation. As for the charge of the particles after dissolution in an aqueous medium, they are classified as cationic (all basic dyes), anionic (direct, acid and, reactive dyes), and non-ionic (dispersed dyes) (YAGUB et al., 2014). The Turquoise Blue (Figure 1) dye is an anionic dye that has copper phthalocyanine as a chromophore group, reactive in terms of its fixation mode and widely used in the textile industry in the coloring of natural or synthetic fibers.

Figure 1- Chemical structure of turquoise blue textile dye

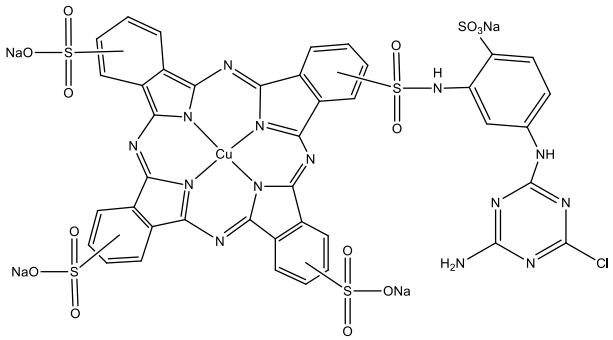

Source: (LEMOS et al., 2023; MACHADO et al., 2015).

The dye used in this work was chosen because it has a metal in its structure, which could participate in the interaction with adsorbents that also have metals in their composition, and may or may not interfere with the adsorption process. Recent studies have shown that this dye can be effectively removed from aqueous media using mixed oxides with a perovskite structure, of the $LaNiO_3$ type, prepared by the proteic method (LEMOS et al., 2023; LEMOS, 2022).

In this sense, this article describes a study of the effect of the type of metal present in the material of the $LaMO_3$ type (M= Mn, Fe, Co, and Ni) on the formation of the perovskite phase, when synthesized by the mechanosynthesis method. In addition, this work also evaluates the feasibility of applying the materials as an adsorbent of dyes in aqueous media with promising results. It is worth mentioning that this article describes the interaction between a dye that has metal in its composition, with with materials with perovskite structure that also have metals, being one of the main novelties of the work, which can trigger new research with other dyes that also have metals in its chemical organization.

EXPERIMENTAL

The preparation of mixed oxides by the method of mechanosynthesis was carried out using a ball mill of the brand Retsch, model PM 100 with three balls with tungsten carbide composition, a diameter of 15 mm and, an average mass of 26 g. A sample vessel of WC with a capacity of 50 mL was used.

For the synthesis of materials such as $LaFeO_3$, $LaCoO_3$ and $LaNiO_3$, La_2O_3 (Vetec, 99.9%) and Fe_2O_3 (Vetec, 99.8%), La_2O_3 (Vetec, 99.9%), and Co_3O_4 (Sigma-Aldrich, 99.5%) and La_2O_3 (Vetec, 99.9%), and Ni_2O_3 (Vetec, 99.9%) were used respectively as starting materials. Masses were weighed in stoichiometric amounts to obtain 4.0 g of the final product. The procedure (LEMOS, 2022) consisted of adding the weighed masses to the grinding vessel, having the powder/sphere mass ratio of 1:20. The vessel/spheres/powder system was rotated at 400 rpm for 6 hours, and every 1.5 hours of grinding there was a 3-minute pause and then the direction inversion. A part of the material obtained in the milling step was placed in a porcelain crucible and subjected to calcination at 10°C min^{-1} until reaching 900°C, remaining for 2 hours.

The same procedures described above were used for the synthesis of the material $LaMnO_3$, however, the starting materials were MnO_2 and La_2O_3. Specifically, in this case, it was necessary to add 10 drops of ammonium oxalate to the powder mixture to promote the reduction of Mn^{4+} to Mn^{3+}. The materials $LaMnO_3$, $LaFeO_3$, $LaCoO_3$ and $LaNiO_3$ synthesized and calcined at 900°C were named as LM-M9, LF-M9, LC-M9 and LN-M9, in that order.

The X-ray diffraction (XRD) pattterns were performed at room temperature using a PANalytical Empyrean X-ray diffractometer with Cu Kα radiation (λ = 1.5406 Å) and Bragg-Brentano geometry in a continuous mode with an angular range $10 \leq 2\theta \leq 60°$ and step size of 0.02°. The identification of the present phases was carried out by comparison with the data from the ICSD (Inorganic Crystal Structure Database) e JCPDS (Joint Committee on Powder Diffraction Standards). Rietveld refinements were performed using the interface DBWS9807-tools (YOUNG et al., 2000). To estimate the average crystallite sizes, it was used the Scherrer equation.

The morphology of the materials obtained were analyzed using Scanning Electron Microscopy (SEM), using a HITACHI model TM 3000 equipment. The zero load point pH (pHPCZ) was determined using the equilibrium method in a batch system, with initial pH values of 3, 5, 7, 9, and 11. The absorbance spectrum of the dye solution and the analytical curve was obtained in an absorption spectrophotometer in the UV-Vis region of the Shimadzu UV-1800. For the absorption spectrum, the scan was applied in the wavelength range between 400 and 700 nm. For the calibration curve, dye solutions with concentrations of 10, 20, 30, 40, and 50 mg L^{-1} were used in triplicate.

Initially, 250 mL of a solution with a concentration of 30 mg L^{-1} of the turquoise blue dye was placed in a beaker, at a temperature of 25°C, under magnetic stirring and the pH was adjusted

to 3.0 with the aid of the HCl solution 0.1 mol L^{-1}. Then, 0.05 g of the adsorbent (previously dried at 60°C for 30 minutes) was inserted and at the determined times of 5, 15, 30, 60, and 90 minutes, an aliquot was removed from the medium, submitted to the separation of the adsorbent solid and the remaining solution was analyzed by absorption spectrophotometry in the UV-Vis region, in the range of 400 to 700 nm. A similar test was also carried out to assess whether the turquoise dye undergoes photodegradation during the tests under the conditions used, but without the addition of the adsorbent. The tests were performed in triplicate. The values of removal efficiency (E) and amount of adsorbed dye (q) in milligrams per gram of adsorbent were calculated based on equations well-known in the literature (LEMOS et al., 2023; LEMOS, 2022). Pseudo-first order (PPO), pseudo-second-order (PSO), and variable constants (CV) kinetic models were used for the kinetic study of adsorption (LEMOS, 2022).

RESULTS AND DISCUSSION

Figure 2 shows the X-ray diffraction patterns and Rietveld refinement results for materials (a) LM-M9, (b) LF-M9, (c) LC-M9, and (d) LN-M9. The solid curves (in red) represent the defaults calculated from the structural model used in Rietveld Refinement to fit the experimental data. The blue lines at the bottom of each XRD pattern correspond to the difference between experimental and calculated data.

The XRD pattern presented in Figure 2a shows intense peaks that correspond to the $LaMnO_3$ perovskite structure with orthorhombic symmetry and Pnma space group (ICSD nº 16-1928). The LM-M9 material also presents a low-intensity peak at 25.72º, referring to a secondary phase of lanthanum oxide La_2O_3 (ICSD nº 25-7585). According to literature data, the $LaMnO_3$ material has six characteristic peaks with positions around 22.80°, 32.40°, 39.90°, 46.50°, 52.30° and 57.70°, which indicates that the material prepared in this work has the same or similar structure to the studied (MOURE; PEÑA, 2016; NASCIMENTO et al., 2021; SOUZA et al., 2021; SANTOS et al., 2019).

The XRD pattern of the LF-M9 material (Figure 2b) indicates the formation of the $LaFeO_3$ perovskite-like structure with orthorhombic symmetry and Pnma space group (ICSD nº 19-4609). The LF-M9 material also showed a peak at 53.43º referring to a secondary phase of lanthanum oxide La_2O_3 (ICSD nº 25-7585). According to the literature, the $LaFeO_3$ material with perovskite structure has six characteristic peaks at 22.60°, 32.20°, 39.70°, 46.20°, 52.10°, and 57.50°, this result was confirmed by comparing the XRD pattern of the material with the same or similar structure to the one studied (MOURE; PEÑA, 2015).

In the XRD pattern of the LC-M9 material (Figure 2c) the formation of more than one crystalline phase is evident. The positions of the Bragg peaks indicate the formation of the $LaCoO_3$ perovskite structure with rhombohedral symmetry and R-3c space group (ICSD n° 23-0644). The characteristic peaks for the $LaCoO_3$ material are reported in the literature at $2\theta = 23.3°$,

32.9°, 33.3°, 40.7°, 47.5°, 53.8° and 59.0° (MOURE; PEÑA, 2015) and are in good agreement with the results observed in this work. In addition, in the XRD pattern, different peak symbols are also highlighted referring to the spinel structure of Co_3O_4 (ICSD nº 29-0720), cobalt(II) oxide CoO (ICSD nº 24-5319) and lanthanum(III) oxide La_2O_3 (ICSD nº 25- 7585). It is also possible to note the presence of some peaks referring to possible spurious phases that were not identified.

For the LN-M9 material (Figure 2d), the positions of the Bragg peaks indicate the predominant formation of the $LaNiO_3$ perovskite structure with rhombohedral symmetry and R-3c space group (JCPDS 33-0711). In addition, it was also observed the presence of low-intensity peaks referring to lanthanum oxide La_2O_3 (ICSD nº 25-7585) and nickel oxide (ICSD nº 25-9699).

Figure 2 - XRD patterns for (a) LM-M9, (b) LF-M9, (c) LC-M9, and (d) LN-M9. The solid curves (in red) are the calculated patterns via Rietveld refinement.

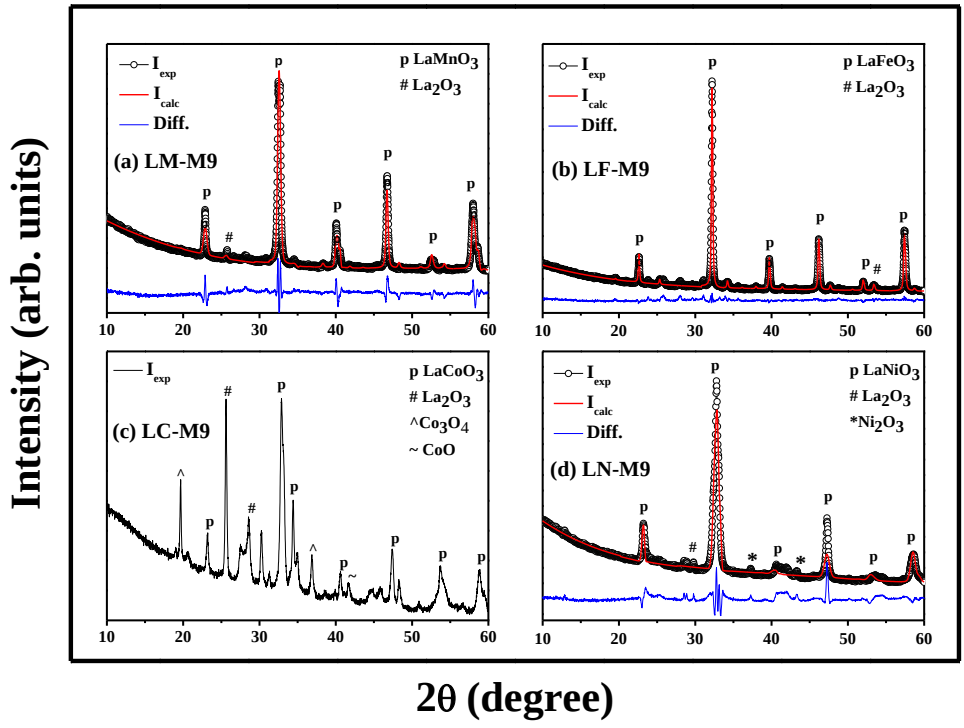

Elaborated by the authors

Observing the XRD patterns of the synthesized materials, it is noted that some of the mixed oxides presented perovskite structures with orthorhombic symmetry, except for $LaNiO_3$, which presented rhombohedral symmetry. It should be noted that the distortion in the structure of the ABO_3 perovskite is quite common and is usually associated with the tolerance factor (t). The ideal cubic structure is formed at t = 1 when the A^{3+} and O^{2-} ions are combined in size to form packed cubic layers, while the B^{3+} cations fit into the interstices formed by the O^{2-} ions to give an octahedral matrix of BO_6. For t<1, the BO_6 octahedron cooperatively tilts to accommodate the

mismatch, forming less symmetrical orthorhombic structures (GRABOWSKA, E., 2016; MOURE; PEÑA, 2015).

The formation of the desired phase with perovskite structure was predominant in all materials prepared with medium to high relative intensity peaks. Despite this, the formation of secondary phases was observed in all materials prepared through a few low-intensity peaks. Although the reagents were mixed in stoichiometric amounts, the use of grinding in a ball mill for 6 hours, followed by calcination at 900°C for 2 hours was not enough to provide total effective contact between the species involved and thus result in the single phase material. Similar results were reported in studies carried out by Santos et al. (2019). In these studies, using the same mill used in this work, but different grinding and calcination conditions than those used in this work, indicated the need to optimize the conditions for obtaining the single-phase material, such as higher calcination temperatures, or longer time on plateau level, besides optimization of the powder/bead ratio in the grinding vessel.

Table 1 presents the values of the network parameters and the volume of the unit cell (**V (Å^3)**) and phase mass percentage (M) obtained from the Rietveld refinement and refers to the predominant phase of each sample. In addition, the values of the average crystallite sizes (D) for the $LaMnO_3$ (LM-M9), $LaFeO_3$ (LF-M9), $LaCoO_3$ (LC-M9), and $LaNiO_3$ (LN-M9) phases of the synthesized materials are also presented.

Table 1 - Data on network parameters, unit cell volume, phase mass percentage (M) the average crystallite size (D) and pHPCZ for the synthesized materials.

Material	**Cell Parameters (Å)**			**V (Å^3)**	**M(%)**	**D (nm)**	**pH$_{PCZ}$**
	a	*b*	*c*				
LM-M9	5.4764(1)	7.7915(6)	5.5249(4)	235.74(8)	93	18	7.2
LF-M9	5.5543(7)	7.8607(2)	5.5545(1)	242.52(7)	99	32	4.4
LC-M9	-	-	-	-	-	9	6.2
LN-M9	5.4826(4)	5.4826(4)	13.3069(7)	346.41(2)	93	7	7.2

Elaborated by the authors

The LM-M9 and LF-M9 materials showed main phase crystallite sizes with values of 18 and 32 nm, respectively. These values are in agreement with data reported in the literature for materials with this type of structure (NASCIMENTO et al., 2021; SOUZA et al., 2021). The crystallite size values for materials with perovskite structure with cobalt in the B site obtained by the stoichiometric mixture of oxides method were similar to those found in this work, whose value was 9 nm, for the LC-M9 material. On the other hand, the LN-M9 material showed a crystallite size of 7 nm. Similar behavior has been reported previously for $LaNiO_3$ perovskite synthesized by the mechanosynthesis method (SANTOS et al., 2019). When analyzing the crystallite sizes

of the synthesized materials, it can be seen that the LN-M9 material is the one with the lowest value, this fact may be related to the size of the ions that make up the B side of the perovskite structure since nickel is the smallest of the studied ions. According to the literature, in general, the average size of the perovskite crystallites is in the range between 13 nm and 40 nm (GARBA et al., 2020; JUNIOR et al., 2018; GRABOWSKA, 2016; MOURE; PEÑA, 2015; NASCIMENTO et al., 2021; LEMOS et al., 2023; SOUZA et al., 2021), so there is consistency and proximity between the results.

The adsorptive processes depend on some factors, among them the pH of the solution and the affinity of the adsorbent with the adsorbate. The surface loads of the adsorbent, which depend on pH, can be easily manipulated with acidic or basic treatments. It is worth mentioning that the knowledge of surface loads is essential to know the best pH for greater retention of residue on the surface of the material. The zero-load point pH (pHPCZ) is the point at which the surface pH of the material is neutral (zero-load). The determination of the same is a very important characteristic to know the behavior of the material according to the amount of H^+ and OH^- present in the solution [46-47]. The zero load point values of the materials LM-M9, LF-M9, LC-M9, and LN-M9 presented in Table 1 are in the range of typically reported in the literature which indicates in the range of 6.2 to 10.9 with lanthanum at site A of materials with perovskite structure (MOURE; PEÑA, 2015; NASCIMENTO et al., 2021; RIBEIRO et al.,2022).

Given the values obtained for the point of zero charges of the synthesized materials, it can be stated that if the pH of the solution is above pHPCZ, the surface of the material will be negatively charged and it will have a greater affinity for adsorption of cations. On the other hand, if the pH of the reaction medium is below the pHPCZ of the material, the surface will be positively charged and the surface will tend to adsorb anions. Thus, as the Turquoise Blue dye is an anionic dye, the pH of the dye solution must have a value lower than pHPCZ, so that the affinity between the adsorbent and the adsorbate is maximized and, consequently, the removal efficiency as well, although this is not is the only factor that will influence the adsorption efficiency.

Scanning Electron Microscopy (SEM) was used to visualize the microstructural analysis of the synthesized materials. Analyzing the SEM images (Figure 3) it is possible to observe that all four synthesized materials present an asymmetric, spongy and, porous surface. In addition, particles exhibit different dimensions and models. These characteristics are desired in an adsorbent material and are relevant because of the adsorption that can occur within the material's pore system.

Figure 3 - Micrographs for LM-M9, LF-M9, LC-M9, and LN-M9 materials.

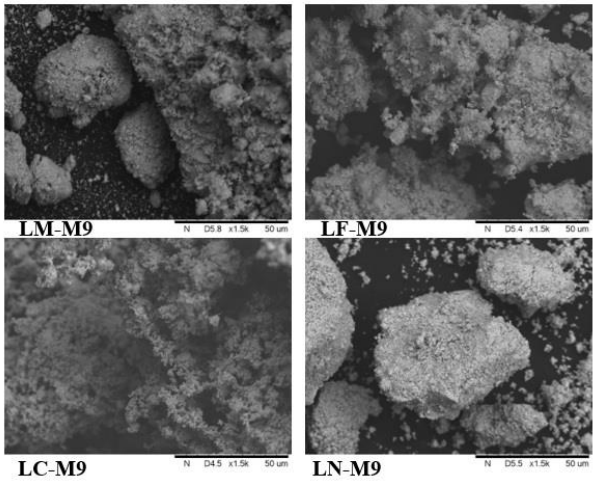

Elaborated by the authors

The adsorption performance can be expressed by the adsorption efficiency, E (%), and the amount of adsorbed dye (q). Concerning to efficiency, it becomes greater as there is a mass transfer from the dye solution to the adsorbent material, thus decreasing its concentration. Figure 4 shows the Turquoise Blue dye removal efficiency as a function of contact time using LM-M9, LF-M9, LC-M9, and LN-M9 materials. It was observed that over time, the concentration of dye in the solution decreases and, consequently the values of adsorption efficiency (E) increase.

Figure 4- Turquoise Blue dye removal efficiency as a function of time using the materials LM-M9, LF-M9, LC-M9 and, LN-M9.

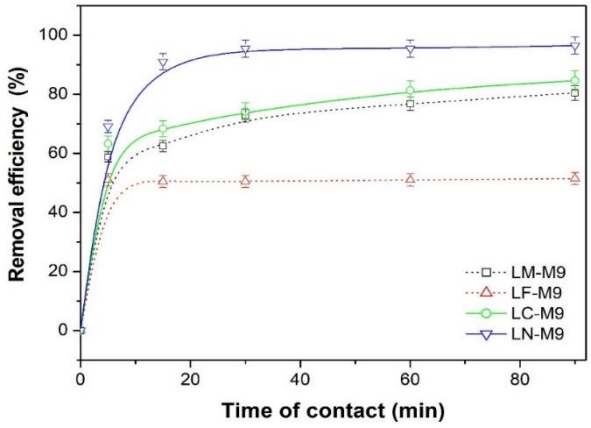

Elaborated by the authors

It is known that in chemical adsorption, generally, the adsorbate molecules can be fragmented, losing their original structure, and dividing into groups, radicals, or molecular ions which are bound to the surface of the adsorbent (GARBA et al., 2020). One can then consider possible coordination between the cations of the B site of the materials with perovskite structure with electron density donor groups present in the Turquoise Blue structure, such as $(SO_3)^-$, whose

coordination points are the oxygens, in addition to the groups (NH_2) and (N=N), where the coordination points are the nitrogen atoms (LEMOS et al., 2023; SOUZA et al., 2021).

The results of a higher percentage of removal, after 30 minutes of contact for most materials, can be explained by the specificity of the interaction, that is, adsorption occurs with greater efficiency with a given adsorbent, as also reported in other works in the literature (NASCIMENTO et al., 2021; LEMOS et al., 2023; SOUZA et al., 2021; SANTOS et al., 2019; RIBEIRO et al., 2022).

When comparing the synthesized materials, the removal efficiency follows the following order: LN-M9 > LC-M9 ≅ LM-M9 > LF-M9. The observed trend may be correlated to several factors, such as average crystallite size, point of zero charges of the adsorbents, and specificity of interaction of the dye adsorption sites with the metal of the B site of the $LaMO_3$-like structure (M = Mn, Fe, Co, and Ni), and material structure. Regarding the aspect of zero load point of the adsorbent and pH of the medium of the adsorption tests, the trend found in the values of removal of the dye from the medium by the different adsorbents can be correlated to the pHPCZ values, where higher pHPCZ values generate a greater difference between the charges of the adsorbent material and the charges of the dye solution, increasing the electrostatic interactions between them (CAO, 2004; LEMOS, 2022).

The $LaNiO_3$ material showed the highest removal efficiency of the turquoise blue dye, about 97% in 30 minutes of testing and it was the material that presented a smaller crystallite size. On the other hand, the material $LaFeO_3$ showed the lowest efficiency of removal of the turquoise blue dye (E = 51%). This material presented the largest crystallite size and its zero charge point is slightly below that typically found for $LaMO_3$-type materials, as reported in the literature. The LM-M9 and LC-M9 materials showed practically the same efficiency value (within the test error margin) and around 80%, although the average crystallite size value of a material ($LaMnO_3$) is about twice on the other ($LaCoO_3$). At first, the results suggest a correlation between removal efficiency values and average crystallite size, at the same time they indicate that this is not the only factor that influences this result. In addition to these aspects discussed, it should also be taken into account that although the perovskite phase of the $LaMO_3$ type is predominant with a mass percentage greater than 90% in most cases, the secondary phases present also have a contribution to the dye removal process in the medium and its removal kinetics.

Several possible forms of interaction between the adsorbent and the dyes are suggested in the literature, such as due to the coordination between the cations of the perovskite structure with electron density donor groups present in the dye structure; due to electrostatic interactions between surface groups of the oxide or cations of the structure with the functional groups of the dye; plus other interactions between the oxide and dye, such as hydrogen bonds and π interactions (GARBA et al., 2020; LEMOS et al., 2023; RIBEIRO et al., 2022).

The use of mixed oxides with a perovskite structure has some advantages as adsorbents for dyes, they have shown a high capacity for removal of dye from aqueous media and typically with relatively fast kinectics, and also possibility of regeneration and reuse with high efficiency maintenance (MANJUNATHAA et al., 2019; GARBA et al., 2020; NASCIMENTO et al., 2021; LEMOS et al., 2023; SOUZA et al., 2021; SANTOS et al., 2019; RIBEIRO et al., 2022). In addition, the material can be prepared with the reduction in synthesis steps and lower calcination temperatures compared to other methods [9, 10, 18, 40, 48]. Studies are still needed to describe the disadvantages of these adsorbents for use in dye removal. It is still necessary to carry out surveys of cost-effectiveness and dependence on various experimental parameters.

The three kinetic models presented high values of linear coefficients, but the kinetic model of constant variables presented coefficients of determination closer to 1. Furthermore, the qav values are closer to the experimental values of adsorption capacity. Thus, it is considered that this model fits better with the adsorption reaction studied (LEMOS, 2022).

When comparing the removal efficiencies of perovskite-type oxides LM-M9, LF-M9, LC-M9, and LN-M9 with works in the literature, it is noted that almost all materials synthesized in this work, except for the material LF-M9, showed similar or greater results than the removal efficiencies of the Turquoise Blue dye using other adsorbents such as MTW zeolite, activated carbon with zinc chloride, TiO_2 or diatomite (MACHADO et al., 2015; RAMESH et al., 2017; AGUEDAL et al., 2018).

Some studies using materials with perovskite structure of type $LaMnO_3$, $LaNiO_3$, $LaCoO_3$, and/or $LaFeO_3$ as adsorbent for dye removal from aqueous media showed that these materials have high efficiency for this application and also can be regenerated after the adsorption of the dye and reutilize. It is noticed that the structure of the perovskite is preserved, this fact can be seen in previous works by using XRD data, which showed that the structure remain unchanged after dye removal. In addition, it is noted that adsorbent without the presence of adsorbed dye can be regenerated through calcination, without changing its initial chemical structure, in addition to being able to be reused while maintaining a high efficiency (NASCIMENTO et al., 2021; LEMOS et al., 2023; SOUZA et al., 2021; RIBEIRO et al., 2022).

CONCLUSIONS

The results obtained showed that it is possible to prepare materials with perovskite structure of the type $LaMnO_3$, $LaFeO_3$, $LaCoO_3$, and $LaNiO_3$ by the milling method with calcination at 900°C, with a phase percentage greater than 90%, whose average size crystallite is in the range of 7 to 32 nm. Obtaining the desired materials was confirmed for all samples, even with the appearance of some secondary phases.

Scanning Electron Microscopy (SEM) through the microstructural analysis of the synthesized materials, showed that the four oxides with perovskite structure in this work have spongy characteristics, with pores and particles of different sizes and models.

The zero load point showed values ranging from 4.4 to 7.2, which could reveal that to adsorb the Blue Turquoise dye, which is an anionic dye, the pH of its solution must have a value lower than the pH of the zero charge point, so that the affinity between the adsorbent and the adsorbate is maximized and consequently the removal efficiency is higher.

The synthesized materials showed removal efficiencies of Turquoise Blue dye in an aqueous solution from 51 to 97%, where the material with nickel in the B site (LN-M9) reached an adsorption efficiency of 97% in 30 minutes of the test.

The results suggest an adsorption specificity of the turquoise blue dye as a function of the metal that composes the B site of the $LaMO_3$ structure (M = Ni, Mn, Fe, and Co) and with the characteristics of the final material obtained. The observed dye removal order LN-M9 > LC-M9 ≅ LM-M9 > LF-M9 is also correlated with the average crystallite size and zero charge point of the adsorbents.

ACKNOWLEDGMENT

The authors acknowledge to CNPq and CAPES for their financial support. This study was financed in part by the Coordenação de Aperfeiçoamento de Pessoal de Nível Superior - Brazil (CAPES) -Finance Code 001. And to CLQM (Center of Multi-users Chemistry Laboratories) from the Federal University of Sergipe for analysis support.

REFERENCES

AGUEDAL, H.; IDDOU, A.; LOCS, J. Optimization of the Adsorption Process of Bezaktiv Turquoise Blue VG Textile Dye onto Diatomite Using the Taguchi Method. **Key Eng. Mater**. v.762, p. 81-86, 2018.

BOLARÍN, A.M.; SÁNCHEZ, F.; PONCE, A.; MARTÍNEZ, E.E. Mechanosynthesis of lanthanum manganite. **Mater. Sci. Eng. A**. v. 454, p.69-74, 2007.

CAO, G. Nanostructures and Nanomaterials, Synthesis, properties ans applications: Imperial College Press, London: 2004.

CONRADI, E.; GONÇALVES, A.C.; SCHWANTES, D.; MANFRIN, J.; SCHILLER, A.; ZIMMERMAN, J.; KLASSEN, G.J.; ZIEMER, G.L. Development of renewable adsorbent from cigarettes for lead removal from water. **J. Environ. Chem. Eng.** v.7, p. 103200, 2019.

CRISTÓBAL, A.A.; BOTTA, P.M.; BERCOFF, P.G.; LÓPEZ, J.M.P. Mechanosynthesis and magnetic properties of nanocrystalline $LaFeO_3$ using different iron oxides. **Mater. Res. Bull.** v,44, p.036-1040, 2009.

DENG, H.; MAO, Z.; XU, H.; ZHANG, L.; ZHONG, Y.; SUI, X. Synthesis of fibrous $LaFeO_3$ perovskite oxide for adsorption of Rhodamine B. **Ecotoxicol. Environ. Saf.** v.168, p. 35-44, 2019.

DOTTO, G.L.; PINTO, L.A.A. Adsorption of food dyes acid blue 9 and food yellow 3 onto chitosan: Stirring rate effect in kinetics and mechanism. **J. Hazard. Mater.** v.197, p. 164-170, 2011.

GALLEGO, J.; MONDRAGON, F.; BATIOT-DUPEYRAT, C. Simultaneous production of hydrogen and carbon nanostructured materials from ethanol over LaNiO3 and LaFeO3 perovskites as catalyst precursors. **Appl. Catal. A.** v.450, p. 73-79, 2013.

GARBA, Z.N.; ZHOU, W.; ZHANG, M; YUAN. Z. A review on the preparation, characterization and potential application of perovskites as adsorbents for wastewater treatment. **Chemosphere** v. 244, p. 125474, 2020.

GRABOWSKA, E. Selected perovskite oxides: Characterization, preparation and photocatalytic properties - A review**Appl. Catal. B.** v. 186, p. 97–126, 2016.

HOLKAR, C.R.; JADHAV, A.J.; PINJARI, D.V.; MAHAMUNI, N.M.A.B.A. J. A critical review on textile wastewater treatments: Possible approaches. **Environ. Manage.** v.182, p. 351-366, 2016.

JÚNIOR, E.M.O.; LEITE, J.O.; SANTOS, A.G.; SOUZA, M.J.B.; GARRIDO PEDROSA, A.M. Nickel-based perovskite catalysts: synthesis and catalytic tests in the production of syngas. **Cerâmica** v.64, p. 436-442, 2018.

LEMOS, J.A.S.; RIBEIRO, I.A.; SOUZA, M.J.B.; GARRIDO PEDROSA, A.M. Evaluation of the Properties of $LaNiO_3$ Material Prepared by the Modified Proteic Method for Adsorption of Environmental Contaminants. **J. Braz. Chem. Soc.** v.34, p. 36-53, 2023.

LEMOS, J.A.S. Estudo da influência dos metais e do método de síntese de materiais com estrutura perovsquita nas propriedades adsortivas em meio líquido. Tese – Programa de Pós-Graduação em Química, Universidade Federal de Sergipe, 2022.

LYU, H.; GAO, B.; HE, F.; ZIMMERMAN, A.R.; DING, C.; HUANG, H.; TANG, J**.** Effects of ball milling on the physicochemical and sorptive properties of biochar: Experimental observations and governing mechanisms. **Environ. Pollut.** v.233, p. 54-63, 2018.

MACHADO, S.W.M.; SANTOS, C.D.; SOUZA, M.J.B.; GARRIDO PEDROSA, A.M. Estudo da remoção do corante têxtil turquesa de efluentes industriais utilizando peneiras moleculares zeolíticas sintéticas. **Scientia Plena** v.11, p. 077201, 2015.

MAHMOODI, N.M.; ARAMI, M. LIMAEE, N.Y.; GHARANJIG, K.; NOURMOHAMMADIAN, F. Nanophotocatalysis using immobilized titanium dioxide nanoparticle. **Mater. Res. Bull**. v. 42, p.797-806, 2007.

MAHMOODI, N.M.; KHORRAMFAR, S.; NAJAFI, F. Amine-functionalized silica nanoparticle: Preparation, characterization and anionic dye removal ability. **Desalination** v. 279, p. 61-68, 2011.

MAHMOUDI, F.; FARHADI, S.; MACHEK, P.; JAROSOVA, M. Phosphotungstic acid supported on silica-coated $LaCoO_3$: Synthesis, characterization and application as a novel and efficient adsorbent for the removal of organic pollutants. **Polyhedron** v.158, p.423-431, 2019.

MANJUNATHAA, C.R.; NAGABHUSHANAA, B.M.; RAGHUB, M.S. PRATIBHAC, S.; DHANANJAYAC, N.; NARAYANA, A. Perovskite lanthanum aluminate nanoparticles applications in antimicrobial activity, . adsorptive removal of Direct Blue 53 dye and fluoride. **Mater. Sci. Eng. C** v. 101, p. 674-685, 2019.

MOHAJERSHOJAEI, K.; MAHMOODI, N.M.; KHOSRAVI, A. Immobilization of laccase enzyme onto titania nanoparticle and decolorization of dyes from single and binary systems. **Biotechnology and Bioprocess Engineering** v.20, p.109-116, 2015

MOURE, C.; PEÑA, O. Recent advances in perovskites: Processing and properties. **Prog. Solid State Chem.** v.43, p.123–148, 2015.

NASCIMENTO, É.V.; GARRIDO PEDROSA, A.M.; SOUZA, M.J.B. Development of $La_xCa_{1-x}MnO_3$ materials for Bezaktiv Blue removal in aqueous media. **Water Sci Technol.** v.83, p. 2793-2808, 2021.

NGAH, W.S.W.; TEONG, L.C.; HANAFIAH, M.A.K.M. Adsorption of dyes and hevy metal ions by chitosan composites: A review. **Carbohydr. Polym**. v.83, p. 1446-1456, 2011.

OVEISI, M.; ASLIA, M.A.; MAHMOODI, N.M. Carbon nanotube based metal-organic framework nanocomposites: Synthesis and their photocatalytic activity for decolorization of colored wastewater. **Inorganica Chimica Acta** v. 487, p. 169–176, 2019.

PALAS, B.; ERSOZ, G.; ATALAY, S. Catalytic wet air oxidation of Reactive Black 5 in the presence of $LaNiO_3$ perovskite catalyst as a green process for azo dye removal. **Chemosphere**, v.209, p. 823-830, 2018.

PALAZON, F.; AJJOURI, Y.E.; BOLINK, H.J. Making by Grinding: Mechanochemistry Boosts the Development of Halide Perovskites and Other Multinary Metal Halides. **Adv. Energy Mater.** v.10, p.1902499, 2020.

PANAHI, P.N.; RASOULIFARD, M.H.; GHOLAMI, Z.; MOHAJER, S. Synthesis of modificated lanthanide nanoperovskites for photocatalytic removal of azo dyes under visible light irradiation. **Int. J. Environ. Anal. Chem**. p. 1-17, 2017.

RAMESH, K.; RAJAPPA, A.; NANDHAKUMAR, V. Z. Adsorption of Turquoise Blue Dye from Aqueous Solution using Microwave Assisted Zinc Chloride Activated Carbon Prepared from Delonix Regia Pods. **Phys. Chem.** v,231, p.1057–1076, 2017.

RIBEIRO, I.A.; LEMOS, J.A.S.; SOUZA, M.J.B.; GARRIDO PEDROSA, A.M. Synthesis of the $LaCoO_3$, $SrCoO_3$ and $La_{0.7}Sr_{0.3}CoO_3$ materials by the modified proteic method and tests for use as adsorbent. **Int. J. Mater. Res.** v.113, 871–88, 2022.

SANTOS, A.G.; LEITE, J.O.; GIMENEZ, I.F.; SOUZA, M.J.B.; GARRIDO PEDROSA, A. M. Effect of the B-site cation from $LaBO_3$ and $LaBO_3/TiO_2$ (B = Mn or Ni) perovskites prepared by mechanosynthesis in adsorption of Congo red dye from aqueous medium. **Mater. Res. Express**. v.6. p.105065, 2019.

SOUZA, A.A.; FERNANDES, J.B.R.; RIBEIRO, J.F.S.; SOUZA, M.J.B. GARRIDO PEDROSA, A.M. Development of $LaMnO_3$ and $LaNiO_3$ type materials with calcium doping by the modified proteic method and evaluation for the dye removal efficiency. **Ceramica** v.67, p. 406-413, 2021.

WANG, Y.; WANG, L.; ZHAO, Y.; YAN, D. Improved luminescence behavior in Er^{3+} doped $KNbO_3$ perovskite structure ceramics. **Ceram. Int**. v.42, p. 17911–17915, 2016.

YAGUB, M.T.; SEN, T.K.; AFROZE, S.; ANG, H.M. Dye and its removal from aqueous solution by adsorption: A review. **Adv. Colloid Interface Sci.** v.209, p 172-184, 2014.

YOUNG, R.A. LARSON, A.C.; PAIVA-SANTOS, C.O. Program DBWS-9807A e Rietveld analysis of X-ray and nêutrons powder diffraction patterns, User's Guide , 2000.

ZHANG, A.; LV, Q. Organic-Inorganic Hybrid Perovskite Nanomaterials: Synthesis and Application. **ChemistrySelect** v.5, p.12641-12659, 2020.